



Improved Power Quality in Battery Chargers for Light Electric Vehicles

Lukka Bhanu Ganesh

Assistant Professor, Department of EEE, Vignan Institute of Technology and Science, Hyderabad, India.

E-mail: bhanuganesh.lukka@gmail.com

K Sujeeth Kumar,

PG Scholar, Department of EEE, Vignan Institute of Technology and Science, Hyderabad, India.

E-mail: sujeethkumar723@gmail.com

Abstract: This work designs and develops a high-efficiency battery charger with high power factor (BL) DC-DC Cuk converters Electric Vehicle (PF). For electric automobiles, it's a lower cost and greater power charge alternative. This charger contains fewer devices in a single switching cycle, which reduces the additional loss of conduction generated by a typical remediator. The efficiency of the loader thereby increases. The recommended architecture also removes undesired capacitive coupling loops and unwanted conduction via the body diode of the inactive switch in the previously designed BL Cuk converters. This significantly increases the charging efficiency. A flyback converter synchronises the constant current commands (CCs and CVs). The recommended loader utilises AC handles to draw a sinusoidal current and the total harmonic distortion (THD) in the supply current is maintained in accordance with IEC 61000-3-2. In order to validate good charging performance under all operating situations, the proposed charger increased efficiency and PQ indicators are tested.

Keywords: BL Cuk converter, flyback converter, total harmonic distortion, Electric Vehicle

I. INTRODUCTION

Battery-powered electric vehicle (BEVs) already outnumber traditional gasoline-powered cars for the long-term growth of the modern transportation industry [1]. An AC-DC converter based on board or off board charger is an important piece of electric vehicle supporting equipment that allows battery charging in BEVs (EV). The literature examines several off-board and on-board topologies of unidirectional or bidirectional EV battery chargers, under level 1 or level 3. A loop charger needs outstanding power quality characteristics (PQ) to lower energy consumption during loading [2]-[4] in addition to its high energy density and a small shape factor. The conventional diode bridge rectifier EV charger (DBR) pulls a high-speed current from the mains, reduces the input power factor (PF) and causes a total harmonic distortion (THD) of up to 55.3%. Table-I provides the electric car test battery rating and the parameters.

Improved PQ-based EV chargers, which draw To solve these difficulties, a sin source current with a more PF and an load voltage that is controlled utilize at a fixed value have been extensively studied in the literature. In recent papers for EV charging, several configurations of front end power factor correction converters are studied, depending on whether they are off-board or on-board. [6] describes a variety of on-board EV chargers, all of which offer the benefits of more power density and efficiency. However, because of the lower vehicle weight and capacity to charge at high power levels, an off-board arrangement is a more feasible alternative. [8-9] describe several PFC converter topologies using interleaved front-end input [7] and the zero voltage switching (ZVS) technique.

A series of BL Cuk converter topologies based on traditional PFC Cuk converters as illustrated in the literature [20-23] discuss (a). The quantities, losses, efficiency, and coupling needs outlined in the next sections have limitations on all these topologies.

As demonstrated in Fig. 2 (b), Topology-1 in [20] has advantages For example, less EMI and facilitating installation, lower input current. The current issue (as illustrated in Fig. 2 (c)) however, is circulating, leading to a further loss in two halves of supply voltage due to the connection of two intermediary condensers, C1 and C2.

Topology-2 employs a significant It A floating terminal is disadvantageous for loading between the two output condensers and a large number of components including the two output condensers. In addition, as shown in Fig. 2 the location of switches for a separate half of the supply voltage, it has the drawback of floating neutral (d).

Topology-3 in [20] is determined to be lossy because the inactive switch S2's body diode is constantly conducting current via Li2 The input voltage was positive half cycle, as seen in Fig. 1; (e).As a result, the current flow through the body diode of the inactive switch is partially returned during another half-cycle operation the circuit constantly suffers some losses across

The Figure 1(f) and (g), which have the same low count of components and lowered the stress on semical device as the usual Cuk converter, are also illustrated in [21] and [23]. Figures 1(f) and 2(g), respectively. Coupling in both the input and output inductors is not feasible with any of these converters. As a result, there may be an increase in The battery life output and input ripple is not optimal.

As a result, in this study, a new power quality enhanced, bridgeless (BL) Cuk converter is presented for EV charging, which matches the approved SAE standard J1772 [26]. The following are the key characteristics of the suggested charger that will help to address the concerns mentioned above.

Because the intermediate capacitors work Circulation losses are independent of both parts avoided, resulting in increased charger efficiency. In the second half cycle there is no back current due to applied control through the body diode from inactive switches. Thus, losses are decreased at the changeover.

Because the PFC converter uses Control is straightforward for every half cycle, the same gate drive and control circuit. The output drives of the proposed cucumber converter are small enough to allow the converter to work in DCM, reducing the cost and size of the converter.

Unlike in Fig. 1(d) is always a ground return path in line voltage in BL operation through Dp and Dn line diodes.

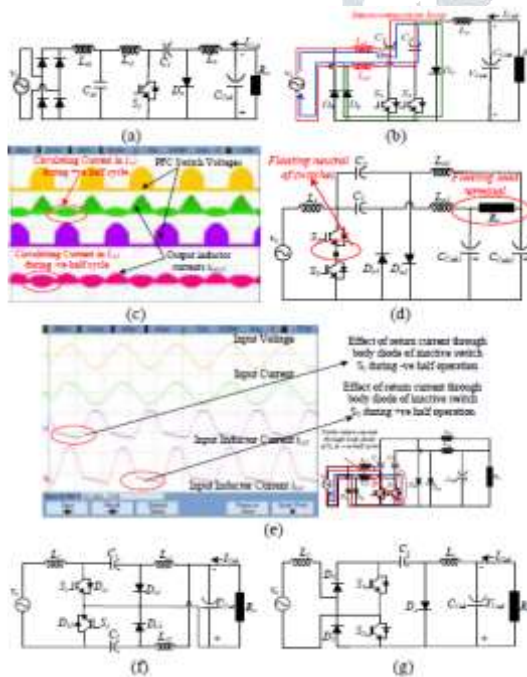


Fig.1. Types of DC-DC BL-Cuk Converter (a) Conventional DC-DC Cuk-Converter (b) Congiguration-1 [20] (c) Current that circulates Because of the topology's linkage between C1 and C2, -1[20] (d) Configuration-2 [20] (e) Configuration-3 with return current [20] through body diode (f) Configuration in [21] (g) Configuration in [23]

II.OPERATION AND CONFIGURATION

Figures 2 and 3 depict the setup and functioning of the proposed Improved EV charger power quality. During a positive half cycle, the Cuk converter cell is made of Li1-S1-Do1-Lo2-Dp. During the negative half line, the second Cuk converter cell, Li2-S2-Do2-Lo2-Dn, is active. The Li1 and

Li2 inductors for both Cuk converter cells work in CCM. The Lo1 and Lo2 output drives are designed, however. in such a way that the output diode current, i_D , is zero after one switching cycle, and the converter enters DCM. The intermediate capacitors C1 and C2 are chosen so that the voltage across the capacitors remains constant during the switching period. It's worth noting that both switches S1 and S2 are controlled by the same PWM signal, lowering system costs and simplifying the circuit.

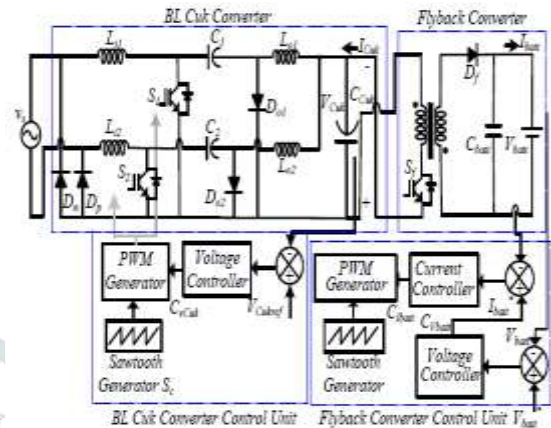


Fig.2 .EV Charger Configuration for BL-Cuk Converter Proposed

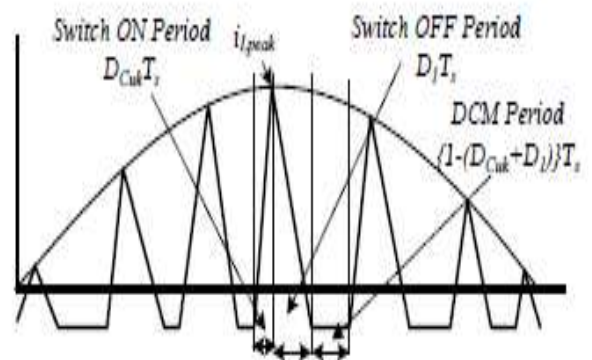


Fig.3. operational principle of power factor correction

Because just A single voltage sensor is used, with a continual use of the single loop voltage feedback control [27-28] to keep the output voltage of the PFC Cuk converter, reducing the cost. The flyback converter is designed to work in DCM[29] with a cascade during the CC (Constant Current) and the CV (Constant Voltage) charging areas. PI controller that handles the battery charging orders.

III.PROPOSED PFC CONVERTER BASED CHARGER DESIGN

A.Design method for proposed PQ

The following is the design method for the Proposed PQ improved 48V/100Ah battery charger. The output voltage of the BL Cuk converter is maintained at 300V constantly. PFC Cuk Converter's voltage gain is derived by the VSPK output voltage, V_{Cuk} and maximum input voltage.

$$M = \frac{V_{Cuk}}{V_{spk}} = \frac{300}{220\sqrt{2}} = 0.964 \tag{22}$$

The value of conduction parameter depends on the inductance L_{eq} , the switching period T_s , and the load resistance R_{Cuk} which is given as follows.

$$K_e = \frac{2L_{eq}}{R_{Cuk}T_s} \tag{23}$$

where 20kHz is chosen as the converter switching frequency ($1/T_s$). The dimensionless parameter K_e is a measure of a converter's proclivity towards discontinuous conduction mode operation. For some duty cycle values, large values of K_e result in continuous mode operation, whereas lower values result in discontinuous mode operation.

Therefore, for DCM operation (24) $K_e < K_{crit}$

As a result, K_{crit} is affected by the kind of converter and the duty cycle D_{cuk} . As a result, the value of the critical conduction parameter K_{crit} is determined as follows to get the border between the conduction and discontinuous conduction modes.

$$K_{e,crit} = \frac{1}{2(M+n)^2} = \frac{1}{2(0.964+1)^2} = 0.1296 \tag{25}$$

For this application, $K_e=0.08$ is chosen for the estimation of different components because the value for DCM is less than the estimated value. The duty cycle is computed as follows for the required output voltage of the Cuk converter:

$$D_{Cuk} = \sqrt{2M\sqrt{K_e}} = 0.384 \tag{26}$$

The converter's equivalent inductance L_{eq} is calculated using (23), as follows:

$$L_{eq} = \frac{K_e R_{Cuk}}{2f_s} = \frac{K_e (V_{Cuk}^2 / P)}{2f_s} = \frac{0.08 \times (300^2 / 850)}{2 \times 20000} = 211.76 \mu H \tag{27}$$

As a result, an equivalent inductance of 200H was used for this application to assure DCM across a large voltage range.

The ripple current in the input inductor is assumed to be 40% to give a constant inductor current during the whole switching cycle. As a result, the input inductance $L_{i1,2}$ is calculated as follows:

$$L_{i1,2} = \frac{V_s \times D_{Cuk}}{\Delta i_{L_{i1,2}} \times f_s} = \frac{220 \times 0.384}{0.4 \times (850 / 311) \times 20000} = 3.86 mH \tag{28}$$

$i_{L1}=0.4 \cdot I_s$, where the peak current ripple is calculated as 40% of the input current. As a result, the input inductance value is set at 4mH to assure CCM functioning.

Now, using (17) and (27) to enable DCM-based functioning, the minimum output inductance $L_{o1,2}$ is calculated as follows:

$$L_{o1,2} \leq \left(\frac{L_{eq} L_{i1,2}}{L_{eq} - L_{i1,2}} \right) = \frac{4 \times 2}{4 - 2} mH = 0.222 mH \tag{29}$$

To guarantee The inductance value of the charger is adjusted below the anticipated level, i.e. 0,15 mH, UPF functioning across the wide input voltage range.

The characteristic of the proposed converter input current waveforming is directly impacted by the energy transfer condenser C1. The design of the condenser is therefore restricted by: The resonant frequency, f_r of L_{i1} , L_{o1} and C1 must exceed line frequency, f during operation of the proposed converter in the respective halves, and f_s , which supply the constant voltage throughout one switching cycle, i.e. $f < f_r < f_s$ such as the switching frequency of converters, f_s , etc.

$$f_r = \frac{1}{2\pi\sqrt{L_{i1,2} + L_{o1,2}} C_{1,2}} \tag{30}$$

In the suggested work, the resonant frequency f_r is set 1.5 kHz. Available. This energy transmission condenser's voltage rating is defined by the sum of the maximum input and output voltages of the charge. Consequently, the energy transfer condenser C1,2 is determined to prevent resonance in each half cycle between C1,2 and L_{eq} .

$$C_{1,2} = \frac{1}{\omega_r^2 (L_{i1,2} + L_{o1,2})} = \frac{1}{(2 \times \pi \times 1500)^2 (4 + 0.15) mH} = 2.71 \mu F \tag{31}$$

To assure CCM functioning, r is set to $2fr$ and The energy transmission condenser value is set to $3F$.

The power consumed from the mains, which includes the ripple power dual frequency (2) component, is calculated as follows:

$$P_i = V_{spk} \sin \omega t \times I_{spk} \sin \omega t = V_s I_s (1 - \cos 2\omega t) \tag{32}$$

The expressions for battery current ripple ($i_{batt r}$) and output ripple voltage (V_{Cuk}) owing to this second harmonic current are as follows:

$$i_{batt_r}(t) = -I_s \cos 2\omega t \tag{33}$$

$$\Delta V_{Cuk} = \frac{1}{C_{Cuk}} \int i_{Cuk}(t) dt = -\frac{I_{Cuk}}{2\omega C_{Cuk}} \sin 2\omega t \tag{34}$$

The The worst-case voltage ripple is determined by the greatest sin value ($2t$), i.e. $t=90$. The DC-link capacitor C_{Cuk} is therefore required to suppress the second harmonic current reef approximated as follows:

$$C_{Cuk} = \frac{I_{Cuk}}{2\omega \Delta V_{Cuk}} = \frac{2.833}{2 \times 314 \times 0.01 \times 300} = 1.5 mF \tag{35}$$

As a result, the output C_{Cuk} condenser in the hardware is adjusted to 2mF, preventing a rated energy second-harmonic current rip and increasing battery life.

IV.MANAGEMENT OF THE PROPOSED EV CHARGER

V. RESULTS AND DISCUSSION

A. Converter control Bridgeless PFC

A. Simulation results and discussion

In discontinuous drive mode with following voltage mode control, the proposed BL PFC convertors are set up. A PI (proportionally-integral) control, which moves the power supplies to match input voltage, guarantees that the BL converter output is consistent, even when the input voltage changes considerably, is used for control of the voltage tracking process. In order to detect any fluctuation in the voltage (V_{Cuk}) caused by a fast shift in the power supply, a voltage sensor is employed. The voltage detected is compared with the required reference voltage (V_{Cukref}). The V_{Cuk} error is received by the voltage feedback controller. At the k th sampling moment, the error signal produced and the control signal are shown as.

The outcomes of the suggested control systems for several test situations are shown in this part. MATLAB 2016 is used for the entire model. Fig 5.2 shows the source voltage, switch1 and switch2 voltage and current waveforms. Source voltage is sinusoidal with peak to peak voltage of 300V. Both the switch voltages are shown in Fig 5, switch voltages are like half wave rectified voltage with twice the magnitude of source peak voltage. Used MOSFET switches for simulation process. Switch current waveforms are shown in Fig 4(d) (e). Both the switches can carry current up to 35A.

$$V_{Cuk}(n) = V_{Cukref}(n) - V_{Cuk}(n) \tag{40}$$

$$C_{vCuk}(n) = C_{vCuk}(n-1) + K_{pCuk}\{V_{Cuk}(n) - V_{Cuk}(n-1)\} + K_{iCuk}V_{Cuk}(n) \tag{41}$$

The EV charger for BL DC-DC Cuk converter is designed for steady state and shown in Fig. The battery voltage battery current source voltage and source currents are recorded for CC mode. Unity power factor can draw from source which shows the in phase to the voltage. from the evident that DC grid voltage is stabled at 290V. The flyback converter is regulated at 65V, it is more than the battery voltage. The entire duration of battery draws 0.1C from the source as shown in the battery current.

The tuned K_{pCuk} and K_{iCuk} are proportional and integral gain constants for the PI controller. A control signal after processing with the PI controller C_{vCuk} is generated, which uses a PWM comparator to vary the duty cycle in order to give the appropriate output voltage. The control signal, C_{vCuk} , is contrasted with S_c , a high frequency wave producing pulses for the BL PFC converter that is internally produced in converter frequency fs:

The voltage, current of the PFC switch S1 and S2 for the half cycles. The proposed BL DC-DC Cuk converter with DC-DC BL converter configuration. The switch currents are no effect with circulating current positive and negative operation. The proposed BL DC-DC converter has does not have circulating current from the waveforms. It improves the efficiency and decrease the power loss. In configuration 1 significant circulating current in both the half cycles. The waveforms are shown in respective figures.

$$\text{for } v_s > 0; \text{ or } v_s < 0; \begin{cases} \text{If } S_c < C_{vCuk} \text{ then } S_{1,2} = 1 \\ \text{If } S_c \geq C_{vCuk} \text{ then } S_{1,2} = 0 \end{cases} \tag{42}$$

The power semiconductor switches voltages, currents of proposed circuit are in safe operation. peak to peak voltage of 590V and current is 29A. the optimal value of inductor selected for continuous conduction mode.

where $S_{1,2}$ indicates the synchronised switching pulses for the proposed BL Cuk converter's two switches S1 and S2. For a broad voltage range, the appropriate duty cycle constraint for the converter, such as the integrated PFC operation, is employed to give a properly controlled DC-link voltage. Compared to other converters based on continuous drive mode, the control approach using a single voltage sensor is found to be relatively straightforward.

The converter performance of Cuk converter and conventional converter as shown in Fig. the capacitor voltage is continues over the switching cycle. The proposed novel converter is good power factor correction for each half cycle. The turn ON of the two switches the current through the inductor. No return current flow from inductor during negative half cycle. The little amount of current flows through the inductor of positive half cycle. The converter efficiency low losses by the diode through the switch.

The suggested control is innovative in that it simplifies the control of the PFC converter by using Each half-cycle has the same gate drive and control circuit. Both S1 and S2 switches operate with a single driving signal in synchronisation. In other words, the inactive diode can reduce conduction

TABLE II. DESIGN RESULTS OF PROPOSED CHARGER

Components	Specifications
Input Inductance, $L_{i,1,2}$	4mH
Output Inductance $L_{o,1,2}$	150μH
Intermediate Capacitor $C_{1,2}$	3μF
Magnetizing Inductance, L_f	130μH
Transformer Turns ratio	0.333
DC-link Capacitor C_{Cuk}	2000μF,400V
Battery Specifications	48V, 100Ah
Charger Output Capacitor C_{Cuk}	2000μF,100V

loss.

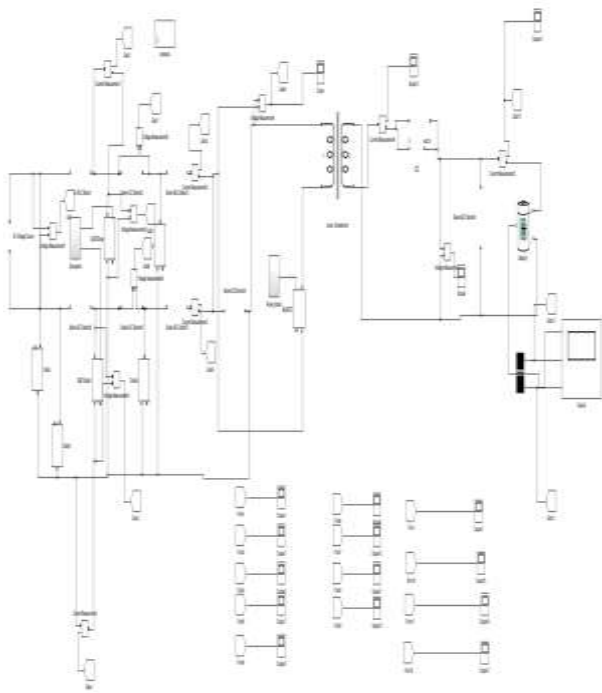
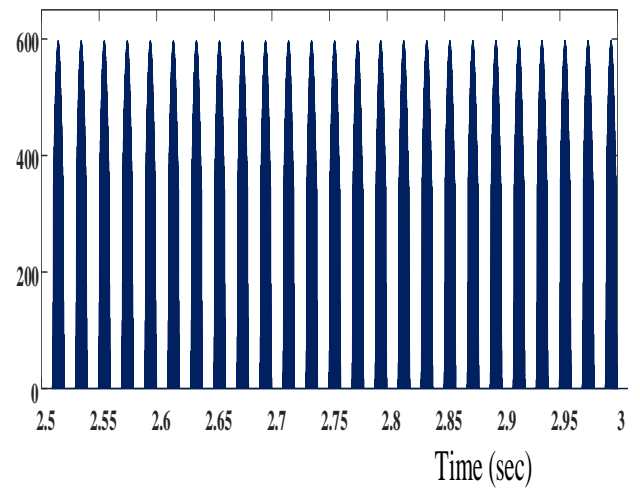
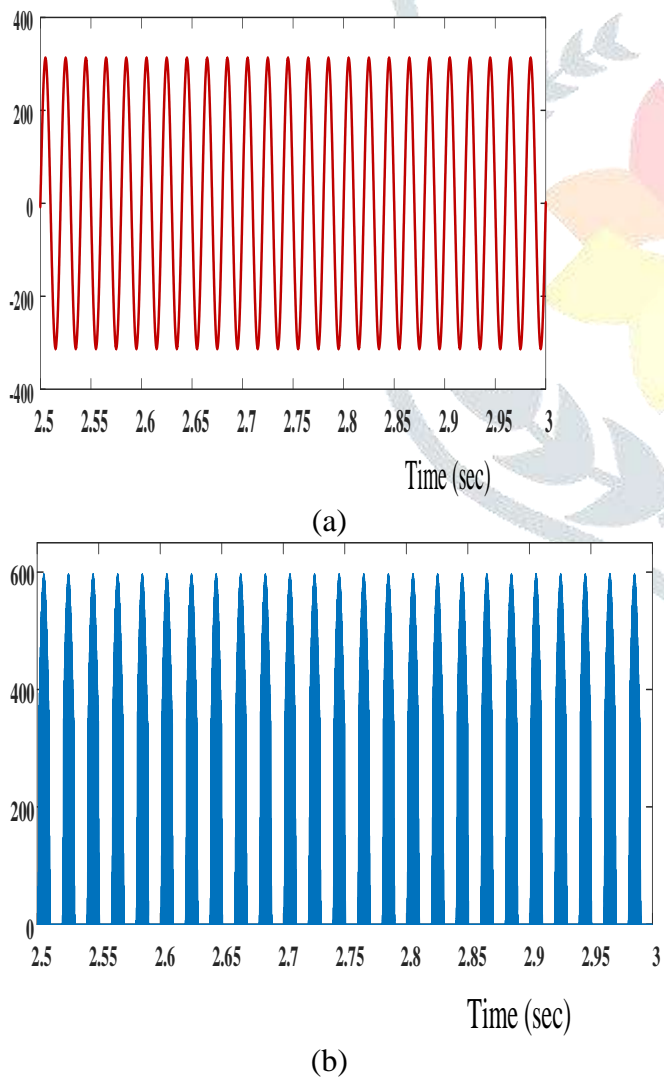
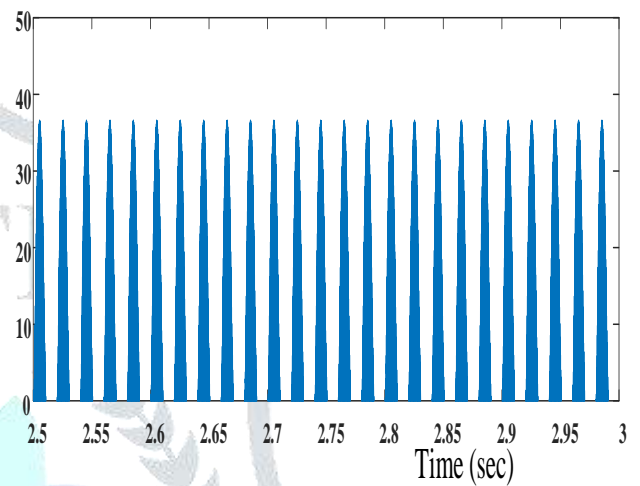


Fig 4. Simulation diagram for BL Cuk converter.

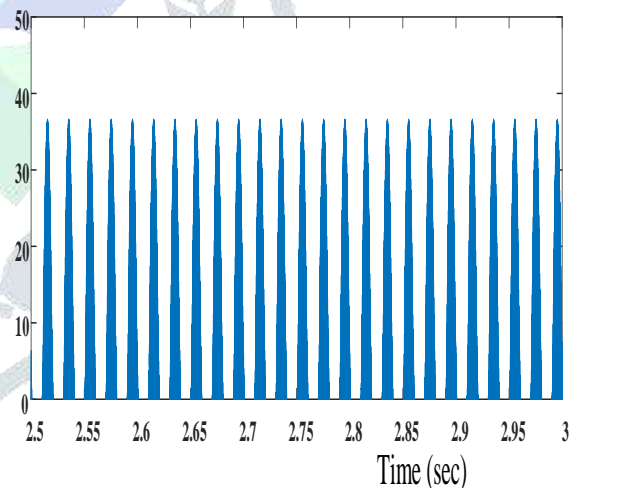
B. Simulation source waveforms



(c)



(d)



(e)

Fig 5. Simulation results for (a) Source voltage (b) Sw1 voltage (c) Sw2 voltage (d) Sw1 current (e) Sw2 current

Variation of input voltage with charge controller rms voltage changeover is introduced in this thesis. The mains voltage from 220V to 105V and return to 105V to 220V. The results are examined and introduced in the Fig. The PI controllers are designed using SISO tool box in MATLAB with phase margin of 60 and bandwidth of 10 krad/sec. This converter rejects transients from source voltage to DC grid voltage of the power factor correction (PFC). Power flow maintain in charge during the period. The main current is sin wave with low THD and bounded operation is created in the source voltage disturbance.

VI. CONCLUSION

With a BL Cuk converter and fewer conducting components during a single switching cycle, It is advised that you enhance the PQ-based EV loader. The suggested PFC Cuk converter delivers good PFC features in DCM mode with a single voltage feedback control. Consequently, the size of the loader is reduced. In this architecture, the unwanted capacitive connection loop and the unwanted conduction of the inactive switch through the body diode are likewise eliminated in the previously constructed BL Cuk converter. This boosts the charger's efficiency substantially. During constant state and during 50% grid voltage variation, the suggested charger demonstrated good charging behaviors. However, the suggested charger's PQ is determined using IEC 61000-3-2 standards across a large input voltage range. As a result, the suggested charger provides a practical EV charging option with enhanced power quality and efficiency.

REFERENCES

1. C. Chan and K. Chau, "Power electronics challenges in electric vehicles," in *Proc. IEEE IECON'93.*, pp. 701–706.
2. B. Tar and A. Fayed, "An overview of the fundamentals of battery chargers," *IEEE MWSCAS'16*, pp. 1-4.
3. M. Yilmaz and P. T. Krein, "Review of battery charger topologies, charging power levels, and infrastructure for plug-in electric and hybrid vehicles," *IEEE Transactions Power Electronics*, vol. 28, no. 5, pp. 2151–2169, May 2013.
4. S. S. Williamson, A. K. Rathore, and F. Musavi, "Industrial electronics for electric transportation: Current state-of-the-art and future challenges," *IEEE Transactions Industrial Electronics*, vol. 62, no. 5, pp. 3021–3032, May 2015.
5. *Limits for Harmonics Current Emissions* (Equipment current per Phase), International standards *IEC 61000-3-2*, 2000. 16A
6. F. Musavi, M. Edington, W. Eberle and W. G. Dunford, "Evaluation and Efficiency Comparison of Front End AC-DC Plug-in Hybrid Charger Topologies," *IEEE Transactions Smart Grid*, vol. 3, no. 1, pp. 413-421, March 2012.
7. H. Choi, "Interleaved Boundary Conduction Mode (BCM) Buck Power Factor Correction (PFC) Converter," *IEEE Transactions Power Electronics*, vol. 28, no. 6, pp. 2629-2634, June 2013.
8. Y. Hsieh, T. Hsueh and H. Yen, "An Interleaved Boost Converter With Zero-Voltage Transition," *IEEE Transactions Power Electronics*, vol. 24, no. 4, pp. 973-978, April 2009.
9. C. Li and D. Xu, "Family of Enhanced ZCS Single-Stage Single-Phase Isolated AC-DC Converter for High-Power High-Voltage DC Supply," *IEEE Trans. Ind Electron.*, vol. 64, no. 5, pp. 3629-3639, May 2017.
10. S. Chen, Z. R. Li and C. Chen, "Analysis and Design of Single-Stage AC/DC SLLC Resonant Converter," *IEEE Transactions Industrial Electronics*, vol. 59, no. 3, pp. 1538-1544, March 2012.